Constrained Sampling Using Simulated Annealing

Azadeh Mohebi and Paul Fieguth

Department of Systems Design Engineering, University of Waterloo
Waterloo, Ontario, Canada, N2L 3G1

Abstract. Scientific image processing involves a variety of problems including image modeling, reconstruction, and synthesis. In this paper we develop a constrained sampling approach for porous media synthesis and reconstruction in order to generate artificial samples of porous media. Our approach is different from current porous media reconstruction methods in which the Gibbs probability distribution is maximized by simulated annealing. We show that the artificial images generated by those methods do not contain the variability that typical samples of random fields are required to have.

1 Introduction

Scientific imaging plays a key role in many research areas such as medical imaging, remote sensing and porous media. Due to the significant research funding and public interest in medical imaging and remote sensing, these aspects have been considered and studied significantly. However, there are other aspects like porous media in which more contributions and attentions are needed. Porous media is the science of water- porous materials such as cement, concrete, cartilage, bone, wood, and soil, with corresponding significance in the construction, medical, and environmental industries[12]. Fig. 1 shows two samples of porous media. Describing and studying the permeability, porosity and transport properties of porous media requires various 2D and/or 3D high-resolution realizations. However, obtaining 2D high-resolution of porous media surface requires cutting, polishing, and exposure to air, all of which may alter the sample, and the process is costly, and 3D samples are generated by MRI imaging which can only resolve large scale structures. Therefore, artificial realizations are required to be generated using *porous media reconstruction* process. Through this process artificial porous media are reconstructed such that they possess the same statistical properties and structures as the real 2D/3D samples [1]. For the purpose of *porous media reconstruction*, we seek a random realization obeying a model. Since the structure and morphology of porous media are complex, stochastic modeling is a proper approach to representing their structures and statistical properties [13].

While simple stochastic image models such as correlation models and spatial variance can be used to model porous media, they are very poor due to the chaotic and complex morphology of these material, and instead for discrete-state problems (porous media images are binary) widely-used Gibbs Random

M. Kamel and A. Campilho (Eds.): ICIAR 2007, LNCS 4633, pp. 198–209, 2007.

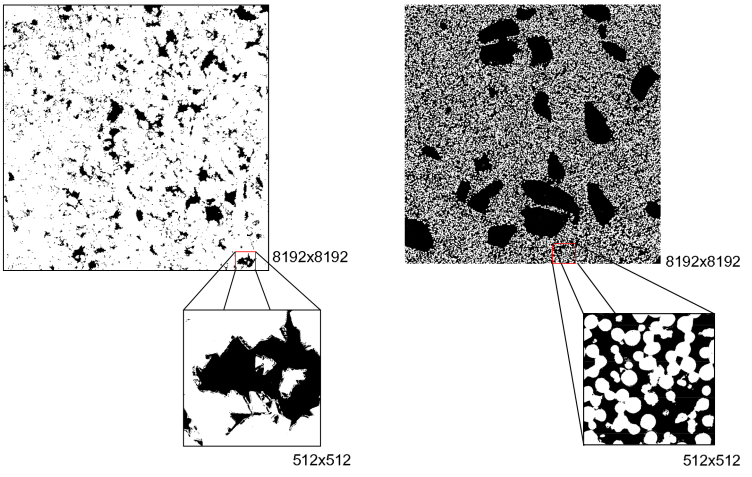

(a) Carbonate Rock (b) Sintered Glass Spheres

Fig. 1. Two Samples of Porous Media. The sample in panel (b) contains large pores known as *vugs*. Porous media have two phases: void and solid, which are presented as black and white, respectively.

Fields(GRF) are considered [8] [16]. GRFs are lattice models, used to quantify the spatial interactions of observed values at the nodes of a grid and to compute a probability for any configuration of that grid [16] [6]. GRFs were originally used in statistical physics to study the thermodynamic characteristics of interacting neighboring particles in a system [16]. For a GRF, Gibbs probability distribution is defined as

$$p(Z) = \frac{e^{-H(Z)/T}}{\mathcal{Z}} \tag{1}$$

for all $Z \in \Omega$ (the configuration space), where $H(\cdot)$ is an energy function written as a function of interactions over a local neighborhood structure, $\mathcal{Z}$ is a normalization factor, and T is the temperature. As the joint prior probability $p(Z)$ is strictly a function of H, the energy H implicitly encodes all of the characteristics of the random field.

Having the prior model defined as (1), the question is how we can use this model to generate artificial samples of porous media. Most people use simulated annealing along with Markov Chain Monte Carlo (MCMC) methods like Gibbs sampler to generate artificial realizations from the Gibbs model [15], [5], [4], [3]. This method involves decreasing T slowly which is equivalent to maximizing Gibbs probability distribution [10]. However, due to the maximization process, the result will be the most probable realization of the configuration space, which can not reflect the variations presented in a typical random sample. This paper propose constrained sampling to generating typical samples from Gibbs probability distribution function (pdf) without maximizing the pdf, and also investigates to what extend the generated typical samples can be representatives of porous media samples.

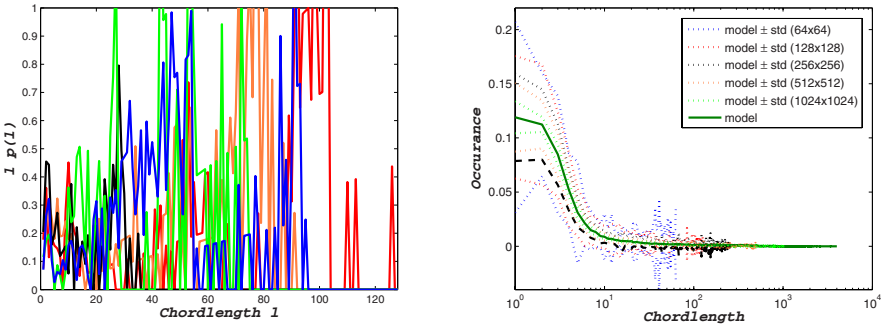

(a) Superimposed chordlength distributions for multiple samples.

(b) Variations in the training sample S at different scales (k).

Fig. 2. Variation of the model with respect to the size of the training sample s_k. Panel (a) shows a set of superimposed chordlength distributions taken from different parts of a large image. Note the considerable variation between samples. For panel (b) we have considered a set of images of size $k \times k$ ($k = 64, 128, 256, 512, 1024$), and inferred the average chordlength probability and its variability as a function of k. Clearly as k decreases the variability increases.

2 Sampling from Gibbs Probability Distribution

Having Gibbs probability distribution defined as (1) we consider chordlength distribution function which is a reasonable widely use function in porous media reconstruction [15], in the energy function. For a two-phase porous media (a binary image), the chordlength distribution function $C^i(\ell)$ is defined to be the probability of finding a chord with length ℓ in phase i. Chords are all line segments between intersections of an infinitely long line thrown in a two-phase random field. The chordlength distribution can be defined for both phases (dual chordlength) and for chords at different orientations. However, we have considered dual chordlength model with horizontal and vertical chords. To define the parameters of chordlength distribution, a training sample S such as those shown in Fig. 1 is used.

The artificial samples generated from Gibbs probability distribution are required to represent the variability in the training sample S. However, S has various structures at different scales. To study the variations in S at different scales, multiple random s_k – truncated images from S at size $k \times k$– have been considered. Each s_k has its corresponding chordlength distribution leading to different energy function. In Fig. 2 panel (a), superimposition of various chordlength distribution for different s_k is shown, and panel (b) shows the variability of chordlength distribution for different k. This variability is due to having different structures at various scales in the training sample S. As can be seen from this figure, smaller k leads to more variability.

The artificial porous media samples need to reflect variabilities presented in the training sample. The method in the literature used to generate artificial

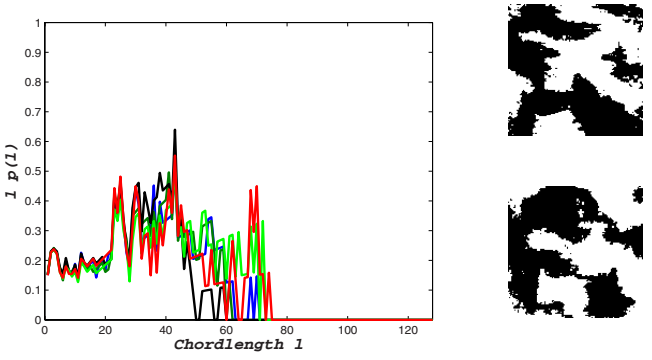

Fig. 3. Superimposed chordlength distributions resulting from annealing down to $T = 0$, with two example images shown. The variation between artificial images is less that the original variation shown in the Fig. 2 panel (a).

samples is simulated annealing [15], [5], [4], [3]. The process of annealing involves generating a sequence of samples through applying the Gibbs sampler and gradually decreasing T in the energy function. This annealing process is started at high temperature, where $p(Z)$ is only a weak function of Z, thus Z is relatively unconstrained, and as T decreases the system is driven to lower energy until the minimum energy, the most probable Z maximizing $p(Z)$, is obtained. However, the images generated by this method can not represent the original variability in the training sample shown in Fig. 2, since T is decreasing down to zero and consequently the probability distribution $p(\cdot)$ is maximized. As shown in Fig. 3, the superimposed chordlength distribution of the generated images through this method are almost the same and do not contain the required variability in comparison to the original variability shown in Fig. 2 panel (a).

Theoretically, for Gibbs sampler to generate independent uniformly distributed random samples from Gibbs probability distribution along with simulated annealing, the relaxation parameter T should be decreased down to a non-zero finite value like $T_f \neq 0$, and the rate of decrease should be logarithmic [10]. However, we do not know at what finite value of T the Gibbs sampler generates independent random sample from the chordlength distribution. Even if T_f can be extracted, the logarithmic annealing schedule causing high computational complexity, should be used to guarantee generating independent random samples, and using fast non-logarithmic schedules leads to *quenching* (rapid cooling), instead of annealing. The small variability in Fig. 3 is due to quenching rather than a typical variability in typical random samples. Quenching is decreasing T faster that the logarithmic schedule, since logarithmic schedule involves very high computational complexity.

Moreover, even if we anneal the energy function down to small enough $T_f \neq 0$ (using logarithmic or non-logarithmic schedule), although large scale structures are presented and there is more variations in the samples (since $p(\cdot)$ is not maximized), the result contains illegal small scale morphologies and structures. Fig. 4 shows superimposed chordlength distribution of the artificial samples generated

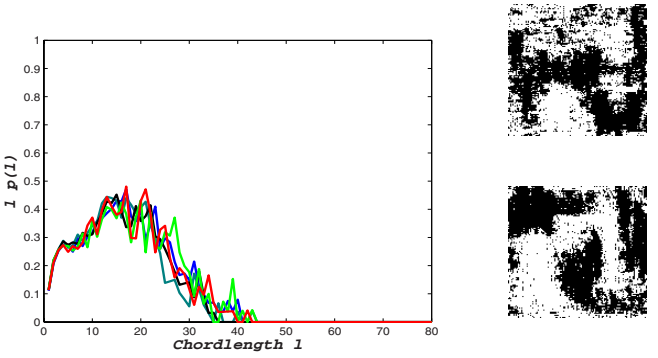

Fig. 4. Superimposed chordlength distributions of samples generated by annealing down to $T_f \neq 0$. Although the variation in small scale structures (small chordlength) is 21% more than the variation of the results generated by annealing down to $T = 0$ in Fig. 3, the samples contain illegal morphologies and structures.

by annealing down to finite temperature T_f. As can be seen from this figure, the variability in small scale structures of the samples generated by annealing down to $T_f \neq 0$ is 21% more than the variability of the results generated by annealing down to $T = 0$.

However, the variability is not inherent in porous media, rather it is a function of scale. As can be seen from Fig. 2, panel (b), as k gets larger, the variability decreases. In general, for $1/f$ (power law, self-similar) [7] processes, there is almost as much as variability in fine scale as in coarse scale, while for ergodic processes such as porous media, there is one scale from which the statistics is stationary. Studying the variability in the training samples at different scales, we can see from Fig. 5 that standard deviation (std) of a set of chordlength distributions obtained from multiple s_k decreases as k increases. Thus, the random field is ergodic from one specific scale (k^*). Therefore to capture the variability in the training sample a possible approach is to synthesize the image at scale k^* – the scale that the ergodicity of the random field is observable.

Thus, for generating random samples, one can

- synthesize an image at size $k^* \times k^*$ by simulated annealing. Since k^* is very large (in Fig. 5 $k^* > 8000$), synthesizing an image at that size involves very high computational complexity.
- consider a smaller scale $k < k^*$, and synthesize the image at that scale by simulated annealing. As discussed earlier and shown in Fig. 3, the results do not represent required variations in porous media.
- down-sample the training sample and synthesize at smaller scale by simulated annealing. By down-sampling the image, we will loose small-scale morphologies information, therefore we can not reconstruct the small scale structures.

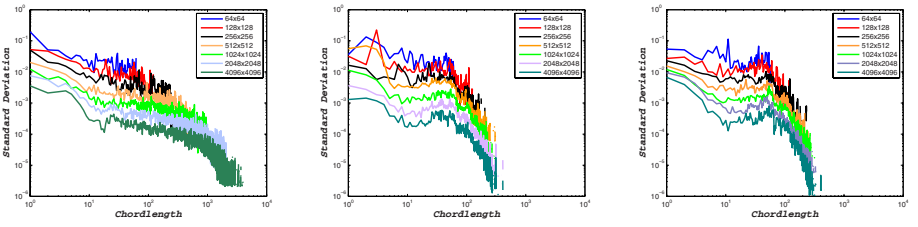

(a) Carbonate rock (b) Sintered glass spheres with vugs (c) Sintered glass spheres without vugs

Fig. 5. Variation of the chordlength model with respect to the size of the training sample having the standard deviation as a function of sample type (a, b, c) and chordlength

- use variable models at different scales and synthesize by simulated annealing. This makes the problem more complicated, and needs an annealing method for variable models.
- use fixed model and synthesize an image at size $k < k^*$ by constrained annealing. Through this approach we propose to change the energy function by adding a constraint. More details on this approach comes in the next section.

3 Proposed Method: Constrained Sampling

To generate typical random samples from Gibbs probability distribution, we propose to

- change the energy function to a constrained energy function,
- generate samples from the constrained energy function using constrained annealing.

3.1 Problem Formulation

The constraint term in the energy function can be measurement (posterior energy function [11]) or another prior model which can take care of invalid small scale structures found in the finite temperature annealing. The constrained energy function is defined as

$$H_c(Z) = H(Z) + \alpha G(Z) \tag{2}$$

where $G(Z)$ is the constraint and α is a parameter controlling the contribution of constraint in the energy function. The constraint term is considered to be another model learnt from the training sample. More specifically,

$$H_c(Z) = \|C^s - C[Z]\| + \alpha \|\mathcal{G}^s - \mathcal{G}(Z)\| \tag{3}$$

where C^s and $\mathcal{G}^s$ are chordlength and histogram [14] distributions respectively, learnt from the training sample, $C[Z]$ denotes the chordlength distribution for Z, and $\|\cdot\|$ denotes ℓ^2-norm.

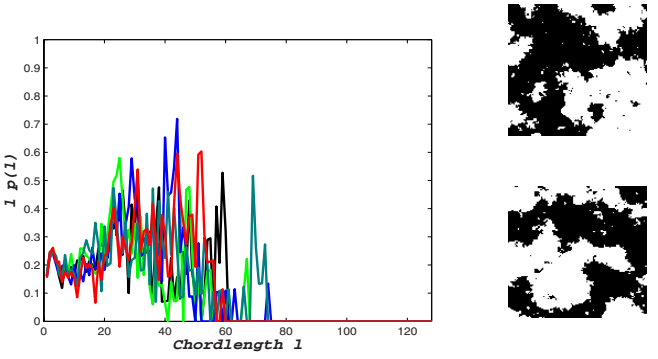

Fig. 6. Constrained sampling by annealing down to finite T and increasing α in equation (2) up to $\alpha_f \neq \infty$. T_f and α_f are set according to the critical phase(Fig. 7), when a steep decrease happens in the energy function. Although the variations in the samples are 22% more than the unconstrained annealing shown in Fig. 3, the samples still contain noisy and invalid structures.

3.2 Methodology

Having the constrained energy function defined as (3), we are required to generate samples. Basically, according to [9], one should fix $T \neq 0$ and increase α up to infinity to satisfy the constraint. However, we do not know what specific value for T leads to porous media samples.

Therefore, we propose to start with large T and small α, and decrease T while increasing α very slowly. This annealing process has a critical phase in which the large-scale structures are generated. Up to this phase both terms in the energy function involve to represent valid structures in the sample. As shown in Fig. 7, by critical phase we mean when a steep decrease happens in the energy function. Fig. 6 shows the samples generated from constrained energy H_c and their variations, right after the critical phase. As can be seen, the variations between samples is more than the variations between images shown in Fig. 3 generated from unconstrained annealing.

After the critical phase, we let T to be fixed (T_f) and let the constraint term changes the medium to small scale structures by continuing increasing α. According to Fig. 3 sampling at T_f from the *unconstrained* energy function in (1) does not lead to a result with valid structures, or we may say that it does not generate porous media samples. With the proposed method, we are sampling at T_f, while the constrained term $G(\cdot)$ contributes in the process from the beginning and after T is fixed, so it can change the small scale structures into the valid structures asserted by the constraint. Therefore, by the proposed method we end up by sampling from the constrained space

$$\{Z|Z \in \Omega, \quad G(Z) = 0\}. \tag{4}$$

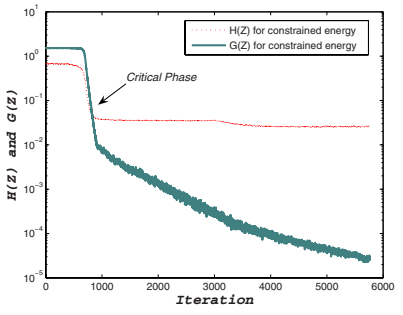

(a) Energy level for constrained and unconstrained energy

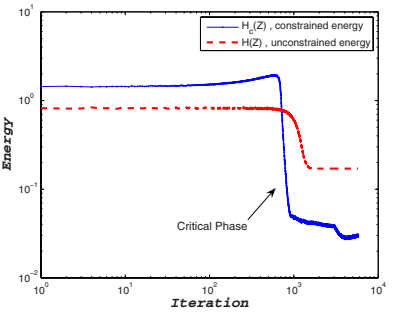

(b) Prior and constrained term in the constrained energy function

Fig. 7. How the energy function changes as a function of iteration. Two methods have been considered here: (1) annealing the unconstrained energy function H down to $T = 0$, and (2) annealing the constrained energy down to T_f while increasing α up to infinity. In both methods there is a steep decrease in the energy function, that we name it as the critical phase. In panel (a) the energy level for both method is illustrated. Panel (b) shows how both terms in the constrained energy (H_c) changes for method (2).

Fig. 8 shows the variability of the samples generated by the proposed method. We can see that the variability is 39% more than Fig. 3.

The proposed method is different from annealing down to $T = 0$ by which the probability distribution is maximized. On the other hand, unlike the results generated by unconstrained annealing, the samples generated by constrained sampling satisfies *two* different prior distribution: $\mathcal{C}^s$ and $\mathcal{G}^s$. Moreover, this approach can be generalized to have more than one constraint in the energy function and changing the parameter for each constraint to control their degree of contribution in the whole process. Although, we can synthesize and reconstruct porous media at smaller scale while having more variations in the samples, for larger image synthesis we still cope with computational complexity, and the original variability in the training sample has not been reached completely.

The proposed method is describe in Algorithm 1. The decrease and increase rate for annealing schedule is considered to be exponential [14].

4 Results and Evaluation

We have considered chordlength distribution for the prior term $H(Z)$ and histogram model as the constraint term $G(Z)$ in the constrained energy function.

The histogram model [14] is non-parametric, keeping the entire joint probability distribution of a local set of pixels within a neighborhood. Choosing eight adjacent pixels as the neighborhood structure leads to a non-parametric model containing of a histogram of $2^9 = 512$ probabilities. The histograms can also be normalized to generate probability mass functions.

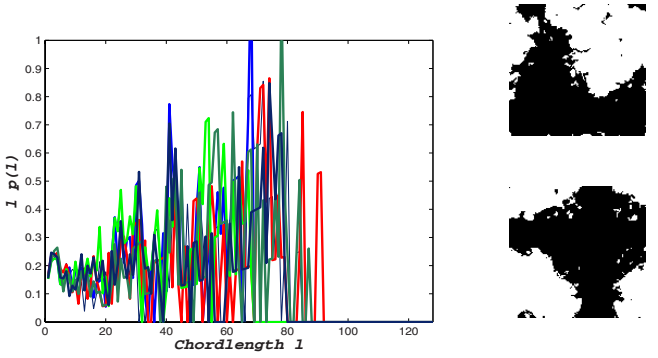

Fig. 8. Constrained sampling by annealing down to finite T_f and increasing α up to infinity. T_f is chosen according to the critical phase, and the algorithm will stop when the constraint in the energy function satisfies, i.e. $G(Z) = 0$. The variations in the samples as shown in the left panel are 39% more than the variations in Fig. 3 obtained by annealing to $T = 0$.

Algorithm 1. Constrained Sampling

```
Start with an initial random field Z_(0)
Initialize T and α
while G(Z) ≠ 0 do
    Update Z_(i+1) from Z_(i) according to Gibbs sampler
    if T < T_f (the critical phase has not passed) then
        Decrease T according to decrease rate
    else
        Let T ← T_f
    end if
    Increase α according to increase rate
    i ← i + 1
end while
```

Fig. 9 shows 256×256 samples generated using constrained sampling.
We evaluate the generated artificial samples in terms of the following criteria

- How much the structures and morphologies presented in the results are consistent with porous media
- How much the results are close to a typical random sample

For the first criterion, we have considered two different porous media models learnt from the training sample s_k at size 128×128 and evaluate the results in terms of those models. We have evaluated the reconstructed images obtained from constrained sampling and unconstrained annealing in terms of histogram model. The evaluation shows that the error for unconstrained annealing (annealing the unconstrained energy down to $T = 0$) in terms of histogram model is 17%, while for constrained sampling it is 3%. The error for unconstrained

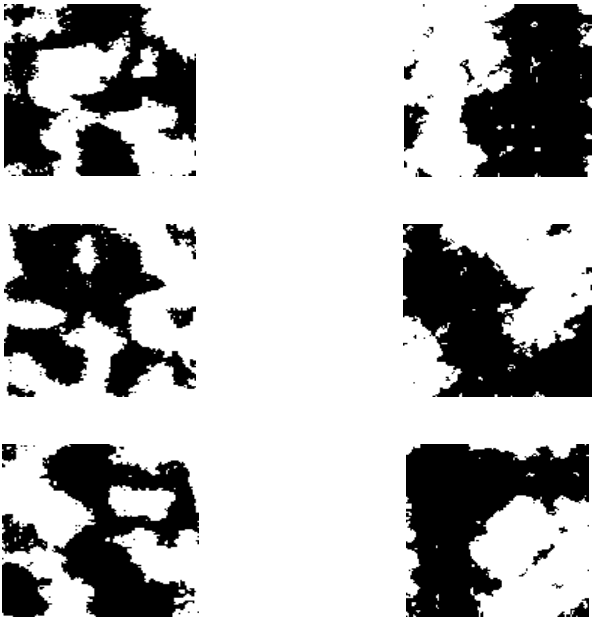

(a) Reconstructed image by annealing the unconstrained energy down to $T = 0$

(b) Reconstructed image using constrained sampling

Fig. 9. Images generated for porous media reconstruction using annealing down to $T = 0$, and constrained sampling

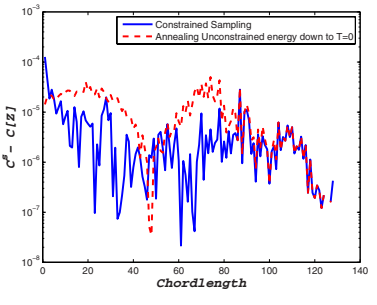

Fig. 10. How much the results are inconsistent to the original sample in terms of chordlength model. The solid and dashed lines show dissimilarity to the chordlength model for the constrained sampling and unconstrained annealing down to $T = 0$, respectively. As the solid-line is closer to zero, the constrained sampling method generates samples which are more similar to porous media samples in terms of chordlength model.

annealing in terms of chordlength model is 0.74%, while for constrained sampling it is 0.06%. Fig. 10 shows how much the reconstructed samples are compatible with the chordlength model learned from the original training sample.

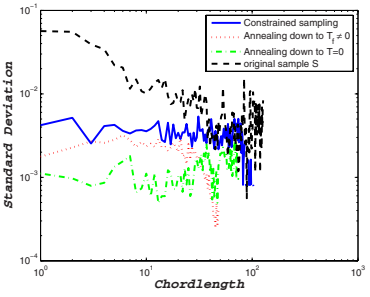

Fig. 11. Comparing the variations in the results in terms of standard deviation. Three different methods have been studied here: (1) annealing the unconstrained energy function H down to $T = 0$, (2) annealing the unconstrained energy function H down to $T_f \neq 0$, and (3) constrained sampling. The standard deviation of the samples generated by each method is illustrated and compared to the standard deviation of the original training sample. The standard deviation of constrained sampling is closer to the original than the others.

For the second criterion, we study the variations in different samples generated by constrained sampling. The variation in samples generated by constrained sampling is more than the other methods, as confirmed in Fig. 11. Although there is variability in the results generated by annealing the unconstrained energy down to $T = 0$, the variability is due to quenching rather than sampling. The proposed approach generate samples with 39% improvement in the variability. However, there is still a difference between the original variability and the proposed method variability.

5 Conclusion

In this paper, an approach for sampling from Gibbs probability distribution is proposed which is based on generating samples from the constrained energy function. The proposed approach is used for porous media reconstruction and synthesis. The previous methods in the literature used for porous media reconstruction is based on maximizing the probability distribution by annealing down to zero temperature, since sampling at finite, non-zero temperature leads to results containing illegal structures and morphologies. These methods generate the most probable realizations which are different from a typical random sample of Gibbs probability distribution, and they can not reflect the scale-to-scale variations in typical samples of porous media. In the proposed method a constraint term is added to the energy function to enable sampling at finite, non-zero temperature while at the same time the generated samples do not contain invalid illegal structures. According to the evaluation results, not only constrained sampling generates samples with 39% more variation than the other method which is based on annealing down to zero temperature, but also the samples are almost ten times more consistent with the original real samples.

References

1. Adler, P.M.: Porous Media, Geometry and Transports. Butterworth-Heinemann series in chemical engineering. Butterworth-Heinemann (1992)
2. Alexander, S., Fieguth, P.: Hierarchical annealing for random image synthesis. In: Rangarajan, A., Figueiredo, M.A.T., Zerubia, J. (eds.) EMMCVPR 2003. LNCS, vol. 2683, Springer, Heidelberg (2003)
3. Torquato, S., Yeong, C.L.Y.: Reconstructing porous media. Physical Review E 57(1), 495–506 (1998)
4. Torquato, S., Yeong, C.L.Y.: Reconstructing random media ii. three-dimensional media from two-dimensional cuts. Physical Review E 58(1), 224–233 (1998)
5. Torquato, S., Manwart, C., Hilfer, R.: Stochastic reconstruction of sandstones. Physical Review E 62(1), 893–899 (2000)
6. Chalmond, B.: The Programming Language Ada. Applied mathematical sciences, vol. 155. Springer, Heidelberg (2003)
7. Falconer, K.J.: Techniques in fractal geometry. Wiley, Chichester (1997)
8. Gelfand, S.B., Mitter, S.K.: Markov Random Fields, Theory and Applications. In: On Sampling Methods and Annealing Algorithms, pp. 499–515. Academic Press, London (1993)
9. Geman, D.: Random fields and inverse problmes in imaging. Lecture Notes in Mathematics, vol. 1427. Springer, Heidelberg (1990)
10. Geman, S., Geman, D.: Stochastic relaxation, gibbs distribution, and teh bayesian restoration of images. IEEE Transaction on Pattern Analysis and Machine Intelligence 6(6) (1984)
11. Mohebi, A., Fieguth, P.: Posterior sampling of scientific images. In: Campilho, A., Kamel, M. (eds.) ICIAR 2006. LNCS, vol. 4141, pp. 365–376. Springer, Heidelberg (2006)
12. Romm, F.: Microporous Media: Synthesis, Properties, and Modelling. Marcel Dekker (2004)
13. Sobczyk, K., Kirkner, D.J.: Stochastic Modelling of Microstructures. Modeling and simulations in science, engineering and technology. Birkhauser (2001)
14. Szu, H., Hartley, R.: Fast simulated annealing. Physic Letters A (122) (1987)
15. Torquato, S.: Random Heterogeneous Materials: Microstructure and Macroscopic Properties. Springer, Heidelberg (2002)
16. Winkler, G.: Image analysis, Random Fileds, and Markov Chain Monte Calro Methods, 2nd edn. Springer, Heidelberg (2003)